



## Design Automation of Lattice-based Customized Orthopedic for Load-bearing Implants

Lorenzo Guariento<sup>1</sup> , Francesco Buonamici<sup>2</sup> , Antonio Marzola<sup>3</sup> , Maurizio Scorianz<sup>4</sup>   
and Yary Volpe<sup>5</sup> 

<sup>1</sup>University of Florence, [lorenzo.guariento@unifi.it](mailto:lorenzo.guariento@unifi.it)

<sup>2</sup>University of Florence, [francesco.buonamici@unifi.it](mailto:francesco.buonamici@unifi.it)

<sup>3</sup>University of Florence, [antonio.marzola@unifi.it](mailto:antonio.marzola@unifi.it)

<sup>4</sup>Careggi Hospital of Florence, [maurizio@scorianz.com](mailto:maurizio@scorianz.com)

<sup>5</sup>University of Florence, [yary.volpe@unifi.it](mailto:yary.volpe@unifi.it)

Corresponding author: Francesco Buonamici, [francesco.buonamici@unifi.it](mailto:francesco.buonamici@unifi.it)

**Abstract.** This work aims at the development of a streamlined and robust CAD procedure to design load-bearing implants. The methodology used to reach this result is explained in the paper: 3D digital anatomy reconstruction of defective structures of the patient is performed with the help of a statistical shape model; subsequently, a CAD modelling tool based on implicit modelling (i.e., nTopology) is used to implement a repeatable semi-automatic procedure that can be performed by a competent user with little effort and limited manual operations. Once that the main shape of the implant is defined, lattice geometries are generated to improve mechanical properties of the implant. The procedure requires as inputs the reconstructed anatomy of the patient and a series of clinical indications on the type of implant that needs to be designed. The paper discusses the development of the whole procedure; achieved results, which include the application of the whole framework on multiple case studies, are presented. The procedure allows the design of a whole implant in 20 minutes circa.

**Keywords:** Custom Implant; Additive Manufacturing, CAD Design Automation, Implicit Modelling, nTopology.

**DOI:** <https://doi.org/10.14733/cadaps.2023.158-173>

### 1 INTRODUCTION

Additive Manufacturing (AM) has emerged as a central factor in the transformation of the healthcare industry, as it has allowed the improvement of patient care in several clinical areas. In orthopedics, surgeons have reduced the invasiveness of surgical interventions, which can now be performed relying on customized tools specifically manufactured for the patient, and have improved the surgical outcome [18]. Patients' safety and satisfaction have consequently seen an increase in the last years [19]. More importantly, because AM allows for the rebuilding of severely

damaged bones and the restoration of joint kinematics that would otherwise be untreatable, it is directly helping to the advancement of the medical field. In this scenario, the diffusion of custom orthopedic prostheses is hindered by the effort required to design such specific devices, whose shape and features are influenced by the patient's anatomy and anamnesis. Indeed, the design phase of such devices is cumbersome and time-consuming, as it involves different human skills (medical and engineering) and resources (medical imaging and 3D modeling software systems). This ultimately leads to a time-consuming process that implies significant costs.

The goal of the present work is to optimize and automate the design phase and 3D modeling of custom orthopedic implants, with the aim of making such devices more and more accessible. Specifically, regarding the automation of orthopedic implant design, an algorithm has been developed within nTopology [46] that is able to generate the 3D model of pelvic prosthesis in  $2 \pm 0.15$  minutes starting from simple CAD inputs. Accordingly, the goal of the present work is to develop a simple and effective tool within the reach of non-expert CAD users, reduce design time and related costs. The paper is organized as follows: Section 2 presents the state of the art on custom implant design: starting from the main workflow, main steps are described and discussed. Section 3 presents the design methodology studied by the authors. Results obtained in this study are finally presented in Section 4.

## 2 STATE OF THE ART

The design process of custom implants can be resumed by the following Fig. 1.

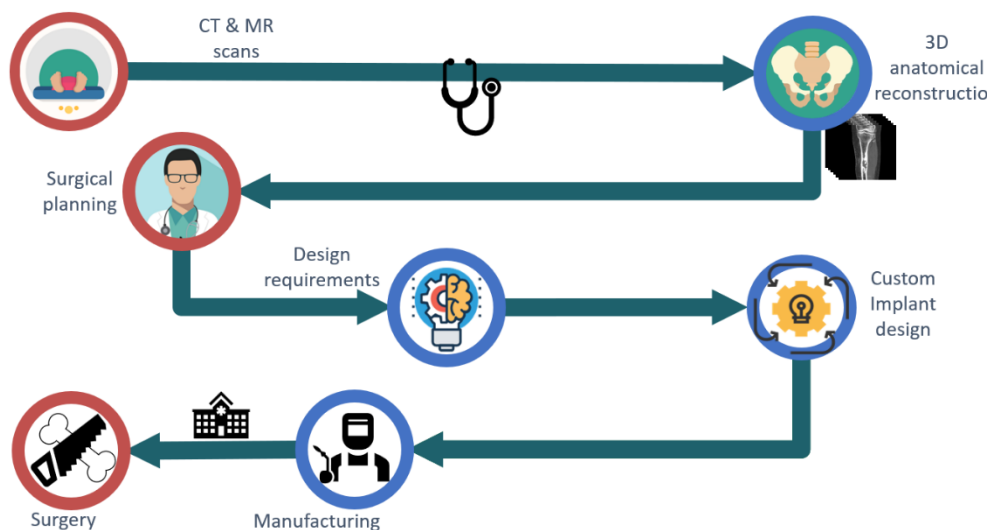


**Figure 1:** Design workflow of custom devices; The operations carried out by clinicians are represented in red, while those demanded to engineers and technicians are highlighted in blue.

The process begins with the generation of the required 3D anatomical models; these are identified and modelled, through a process called segmentation, from the diagnostic images of the patient; dedicated software is used to attain this result. Such models are used to plan the surgery and identify constraints that need to be enforced. Because various severe biomechanical and technological issues must be taken into account, this is by far the most time-consuming procedure. As a result, several iterations are often required before the final design is accomplished. A continuous confrontation between surgeons and engineers is typically required to design a product that is effective and well-built. When designing load-bearing implants that will face severe load conditions or will require an extreme optimization in terms of mass reduction, Finite Element (FE)

Analysis can be performed to evaluate the interaction of the device with the surrounding tissues. However, this step is highly time-consuming and conflicts with the need to achieve the final design of the prosthesis as soon as possible, especially when dealing with oncological cases, which impose a narrow temporal window to counter cancer's advance. The final step of the process is, evidently, manufacturing; depending on the shape of the device and the technology, occasionally some modifications are required, even in this phase, to improve the quality of the product.

The development of tools automatizing the design process could deliver significant advantages in terms of safety and reliability, as they could provide structure to a process that, nowadays, could be considered almost artisanal. Moreover, by reducing the time spent in the modelling phase, more resources could be spent for structural analyses, achieving a higher optimization of the design.

Ultimately, the goal is to make the design and production of custom orthopedic implants more efficient and accessible for patients. The design automation also delivers significant advantages in terms of product safety and reliability; in addition, by reducing the time associated with implant's modeling, more resources can be spent on FE analysis for a deeper biomechanical evaluation of the system and further optimize the design. This work focuses on pelvic implants to tackle the challenges introduced by the complex anatomical structure as well as the presence of numerous vital structures [6]. Nevertheless, the principles exposed in this work can be easily transferred to other anatomical districts.

In order to improve the current design strategy for orthopedic implants, where lattice structures are limited to a few millimeters at the bone-implant interface for osseointegration, in this work the devices are designed with an internal Gyroid-based lattice structure [14], which exhibits promising features for load bearing applications. The introduction of the lattice structure, besides mass and cost reduction, has the positive effect to match the global stiffness of the implant with that of the bone, thus mitigating bone remodeling effect due to stress-shielding [3,35], and providing a biomimetic environment which promotes osseointegration.

## 2.1 Gyroid for Load-bearing Application

An efficient method to decrease the elastic modulus of a metal body, and thus the mechanical mismatch between implant and bone, is to create a lattice infill [24,15,43,38]. Recent developments in Computer Aided Technologies (CAx) and AM allow to model and manufacture porous lightweight cellular metallic structures [5,10,32,41] which exhibit a lower elastic modulus compared to the bulk material. A lattice structure leads to several advantages:

- Mass reduction, and thus weight and cost;
- Possibility to tune the geometric, and consequently mechanical, properties;
- Promote bone ingrowth, providing a stable biological fixation.

It is fundamental that the designed lattice provides a biomimetic mechanical environment that promotes cell migration and seeding [41]. Cell viability, seeding and proliferation are sensitive to the 3D structure of the scaffold, thus it is crucial to mimic the natural architecture of the bone to promote the integration of the host tissue within the implant [31]. Besides the geometry, a mechanical stimulation of the cells as close as the natural condition as possible is beneficial [17,34,44].

Besides stress-shielding mitigation, osseointegration is a key factor for a long-lasting orthopedic implant. Osseointegration is defined as a direct structural and functional connection between ordered, living bone and the surface of a load-carrying implant [28]; thus, bone grows into the porous structure creating a very strong bond between bone and implant. Bone ingrowth into an implanted structure is affected by a multitude of factors, including material microarchitecture, e.g. cell topology, porosity, pore shape and size, and properties of the constituent material [22].

The scaffolds suitable for tissue engineering should satisfy the following structural requirements for an optimal integration with the host bone:

- the scaffold architecture should structurally and functionally mimic the structural hierarchy of the host tissue [23];

- the scaffold must be porous with interconnected pores to provide a viable space for cells, facilitate the diffusion of nutrients and waste products from the implant, and enhance vascularization [7,20];
- the pores should be interconnected to allow Material transport and cell migration [27];
- the pores should have curved cross-sections and avoid straight edges To mimic the curved partitions that separate cells aggregates [42];
- the scaffold should retain its structure after implantation without undesired deformations [13,33];
- the permeability of the scaffold must facilitate the inflow of nutrients and the disposal of metabolic waste [21] through the scaffold's pores.

An orthopedic implant should be designed to guarantee a stable fixation with the host bone and limit stress shielding effects, while ensuring its structural integrity for its life-cycle.

Biocompatible metal materials as stainless steel, Co-Cr alloys and titanium alloys are widely employed for orthopedic applications [39], though the mismatch between Young's modulus e.g. of titanium ( $E = 100 - 110$  GPa) and host bone ( $E = 5 - 30$  GPa) has a negative effect over stress shielding. The most promising approach to tackle this issue is to match the elastic modulus of the implant with that of the bone by implementing a lattice infill, while maintaining an adequate mechanical resistance to static and repetitive loads.

A variety of methods have been developed to produce porous metallic scaffolds with a homogeneous pore size distribution that provides a high degree of interconnected porosity for bone ingrowth [2]. Most popular lattices for bone replacement are:

- Strut-based cellular solids (ordered or stochastic, mimicking trabecular bone)
- Triply Periodic Minimal Surface (TPMS) based cellular solids

In the past decades, a broad variety of lattice structures for orthopedic applications have been tested, such as diamond, truncated cube, truncated cuboctahedron and tetrahedron [43]. Among them, recently the TPMSs have proven to be the most suitable for the discussed application [35,32,45]. TPMSs are a class of implicit surfaces which have often been observed in nature, as in biological membranes [29,26]. TPMSs structures have smooth boundless surfaces that divide the space into two labyrinths in the absence of self-intersections [40]. Compared to strut-based lattices like cubic, octahedral, kelvin etc., these surfaces can guarantee a better biological fixation because they promote a stronger cell adhesion and vascularization [30,4]. TPMS-based cellular structures are characterized by a smoother transition at the connection point of the structure's components compared to strut-based cellular structures [26], which also reduces stress concentrations. The materials' surface characteristics affect the osteoblast adhesion on biomaterials, a fundamental premise for bone integration; therefore, the porosity, pore shape and pore size of the biomaterial play a critical role in the bone ingrowth in vivo [24]. Several studies have proved that porous scaffolds with mathematically designed TPMSs provide a suitable environment for cell adhesion and proliferation [41]. Osseointegration, and thus a stable fixation between bone and implant, is the result of a combination of physiological processes which are highly dependent to some characteristics of the lattice structure: (i) pore size, (ii) pore architecture, and (iii) surface area to volume ratio (SA/V ratio). The main advantage of minimal surface biomimetic scaffolds is the open cell structure, deemed to facilitate cell migration and vitalization, while retaining a high structural stiffness.

Among the TPMSs surfaces, the Gyroid (Figure 2) provides a higher SA/V ratio compared to strut-based lattices [41], which have been proved to promote cell adhesion and proliferation. Gyroid surface has neither planes of symmetry nor straight lines, with a similar topology to the trabecular bone, and allows to create high-performance lattice structures [36,37].

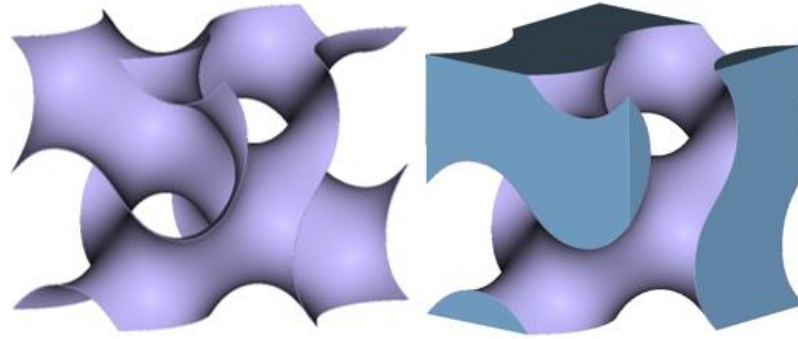


**Figure 2:** Gyroid surface. (a) Gyroid surface, (b) solid Gyroid.

TPMSs can be mathematically modelled with simple implicit functions, and their geometry can be altered in R3 space with no discontinuities or sharp edges [41,45,1], which has a positive effect in reducing stress concentrations. Moreover, thanks to this property, the design process of implants is simplified and easy to control; specifically, the designer benefits from a higher freedom that can be exploited to improve the performances of the prosthesis. Furthermore, TPMS structures have features that maximize their manufacturability via powder-based AM processes [45,29]. Struct-based geometries typically show an excess of sintered material in the nodes of the structure and higher deviation from the desired geometry, with respect to TPMS surfaces [4]. Gyroid proved to be one of the most promising lattice structures for orthopedic applications thanks to its geometric and mechanical properties, as well as its manufacturability via AM.

### 3 DESIGN AUTOMATION

Several case studies, provided by the department of oncological orthopedics of Careggi Hospital have been analyzed to get an insight of the design process of a custom pelvic implant and find the repetitive operations to be optimized and automated. 20 case studies have been considered, which included a wide variety of oncological cases as well as revision implants. The design process can be summarized as follows:

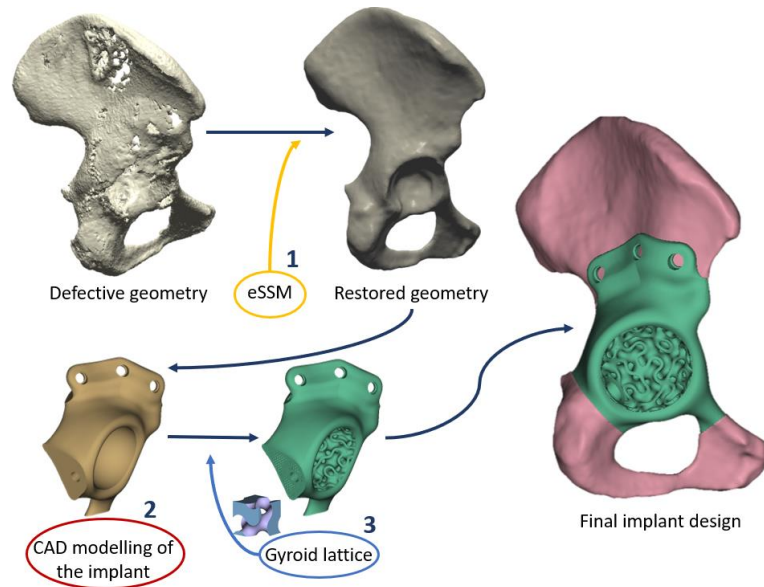
1. Virtual anatomical reconstruction (acetabular parameters, mesh repair)
2. CAD modelling of the implant shape
3. Lattice infill design

Figure 3 resumes these three phases.

The first area of intervention was the development of an automatic workflow for virtual anatomical reconstruction, named eSSM (enhanced Statistical Shape Model) [25], based on Statistical Shape Analysis, which is able to restore highly defective anatomies with no effort, with a great advantage in terms of time; followed the implementation of a series of CAD algorithms for implant design automation and Gyroid lattice infill creation.

#### 3.1 e-SSM

In most oncological cases the target anatomy might be severely damaged and deformed by the pathology. Since the primary function of a pelvic implant is the limb functionality restoration, in most cases the implant doesn't reproduce the exact original anatomy; conversely, the acetabular region receives more importance to ensure satisfaction of functional requirements. An example is provided by Figure 4, where the pelvic implant only restores the acetabulum, while the original anatomy has been neglected.



**Figure 3:** Three steps for custom implant design.

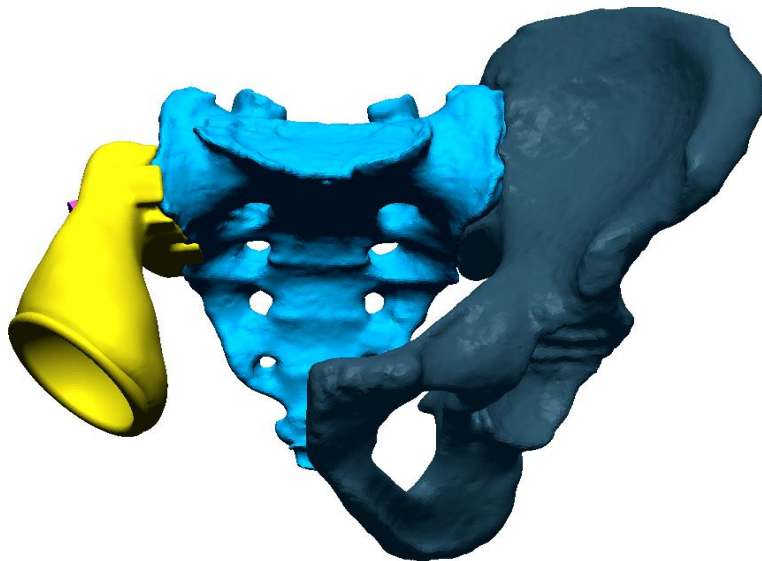


**Figure 4:** Pelvic implant where the original anatomy is neglected, and only the acetabulum has been restored.

In case of large bone defects, in particular when the articular Center Of Rotation (COR) is no longer in its natural location, the very first operation is to retrieve the right acetabular center and orientation in order to guarantee adequate leg length and limb kinematics. The acetabular COR and orientation are defined as the coordinates of the center of rotation of the hip joint, and the orientation of the plane through the acetabular rim, as depicted in Figure 5.



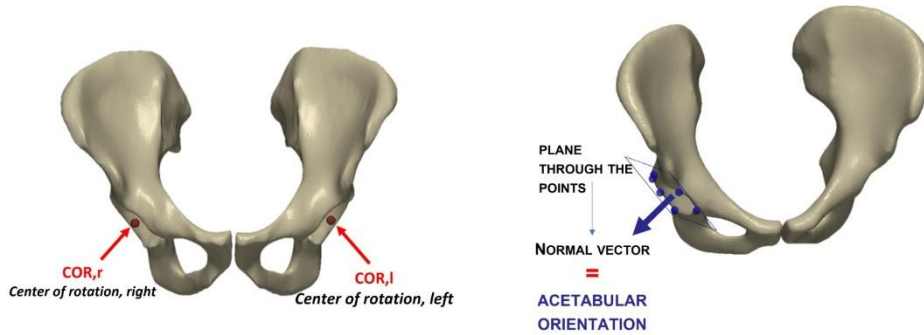


**Figure 5:** Acetabular COR and orientation.

Typically, the COR and acetabular orientation are calculated by expert users by mirroring the healthy COR, whenever possible, though is a time-consuming and error-prone operation. Moreover, in case of large bone defects, like the one in Figure 6, the anatomical model must be manipulated and corrected to obtain a reference geometry for implant design.

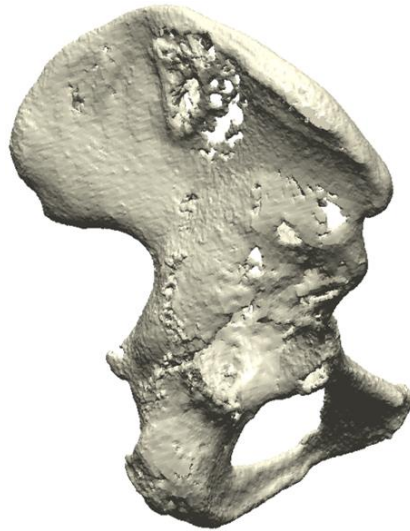


**Figure 6:** Hemipelvis with large bone deficiencies and deformed COR.

With the objective of implant design automation, an automatic tool for anatomical reconstruction have been developed, based on Statistical Shape Analysis. Statistical Shape Analysis (SSA) [11,8,9,16] is an established method widely employed to provide a quantitative description of the geometrical characteristics of a specific family of shapes. When applied to the study of anatomical shapes, SSA allows to synthesize and analyze the information provided by a training set composed by an adequate number of healthy samples of the region of interest (ROI). In its classical formulation, SSA works on a set of training samples provided as discrete models (usually, Point Distribution Models – PDM [16]): the training dataset is then defined as the list of the spatial coordinates of each point of the samples. By assuming all the training samples to be in correspondence (i.e., analogous points are reported in the same positions), SSA exploits powerful mathematical tools, such as multivariate statistical analysis, to interpret and synthesize the information delivered by the training dataset about the possible shape variations from a mean

shape. SSA results in a generative parametric model, usually referred to as Statistical Shape Model (SSM), able to describe the family of shapes under consideration and to “summarize” them under a parametric model.

Indeed, the design of patient-specific devices would be made easier by an access to a collection of statistical information of geometrical descriptors and landmarks of the ROI that goes beyond the mere surface data. Such database would increase the efficiency of the design process by providing easy-to-access information on various geometric characteristics, improving the typical approach which only exploits surface information.

In the application scenario considered, the pelvis, the use of an enhanced SSM (eSSM) would be beneficial whenever the anatomical structure of the acetabulum is severely damaged, and an implant is required. In such cases, the first step is typically the retrieval of the missing geometry and the computation of the natural articular Center Of Rotation (COR) to restore the limb functionality. While the first operation can be affectively carried out automatically by a typical SSA (which calculates the missing geometry according to the highest probability), manual operations are required to retrieve the COR [12]. When the contralateral acetabulum is healthy the most common approach is to mirror its COR, though such method fails when an implant or a bi-lateral defect is present; in addition, the mirroring approach is an important approximation, since the symmetry in human anatomy is only an abstraction and a perfectly symmetric anatomy does not actually exist. The use of an eSSM makes this step automatic, by building an SSM that encompasses the positions of the CORs as learned from the dataset.

The information enclosed within the eSSM presented in the following, are namely the articular centers of rotation and the acetabular orientation. The developed eSSM has been tested over severely damaged anatomies not belonging to the training set and delivered consistent results with a good approximation. A representative example is depicted in Figure 7.

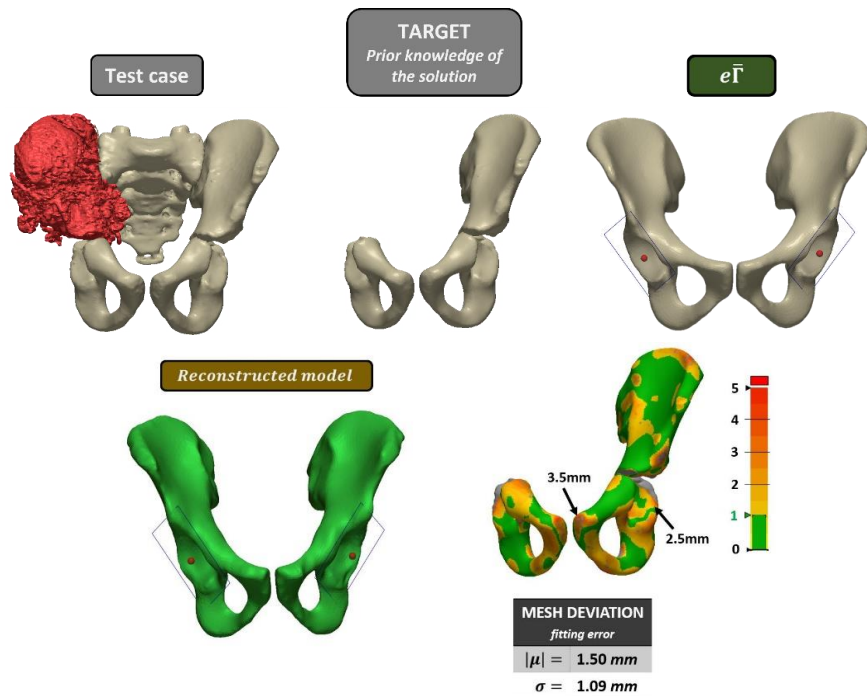


**Figure 7:** eSSM applied to reconstruct a highly defective pelvis.



In the presented example a highly defective pelvis was considered. The eSSM managed to automatically reconstruct a coherent shape with an average error of 1.5mm, which is adequate for the application, along with the acetabular COR and orientation. The reconstruction accuracy can be further improved by increasing the training set number, which to date is composed of 50 pelvic models.

The repaired mesh and the acetabular COR and orientation will be used as inputs for the next phase of implant design; in particular, the polygonal mesh will be used to define the coarse implant's external shape, while the acetabular coordinates will drive the design of the acetabular cup.

### 3.2 CAD Automation

The CAD workflow, implemented in nTopology® [46] is designed to require few inputs and allows for a high design flexibility, in order to cover a broad range of cases. To better understand the type of device that is considered in this study, as well as, the clinical inputs required for its design, the reader can refer to Figure 8. With the support of experienced physicians from Careggi hospital, the three most common types of pelvic implant have been identified, represented in Figure 9.

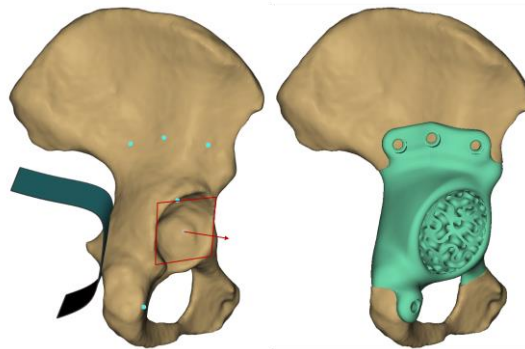


**Figure 8:** (a) required inputs for the automatic procedure for pelvic implants, (b) resulting pelvic implant.

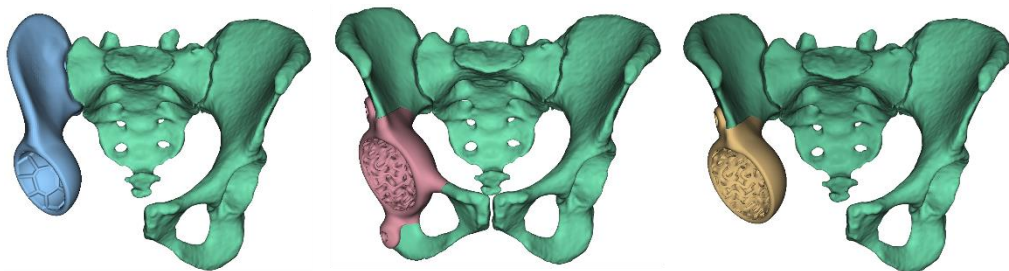


**Figure 9:** (a) Hemipelvic implant, (b) acetabular implant, (c) acetabular implant with removal of pelvic ring.

The first example depicted, Figure 9 (a), represents a hemipelvic implant; among the cases considered, is the most invasive and, due to its typical large dimensions, the lattice infill is not easily applicable for manufacturing issues, mainly for the non-sintered powder removal. The second and third cases, Figure 9 (b), Figure 9 (c) can be manufactured with a lattice internal structure instead.

For this application, an algorithm has been developed within nTopology which encloses the repetitive CAD operations required, taking as inputs the polygonal mesh of the target bone, the resection planes, the acetabular parameters, namely articular Center of Rotation (COR) and acetabular orientation, a set of points corresponding to the location of the fixation screws and, whenever required, a set of CAD surfaces to trim undesired portions of the original bone. The user only has to set the desired values for the design variables, as flange height and thickness, dimensions of the acetabulum and lattice parameters, and the software delivers a ready-to-manufacture 3D model of the implant. Figure 10 shows the implemented graphic interface of the custom function in the nTopology environment.

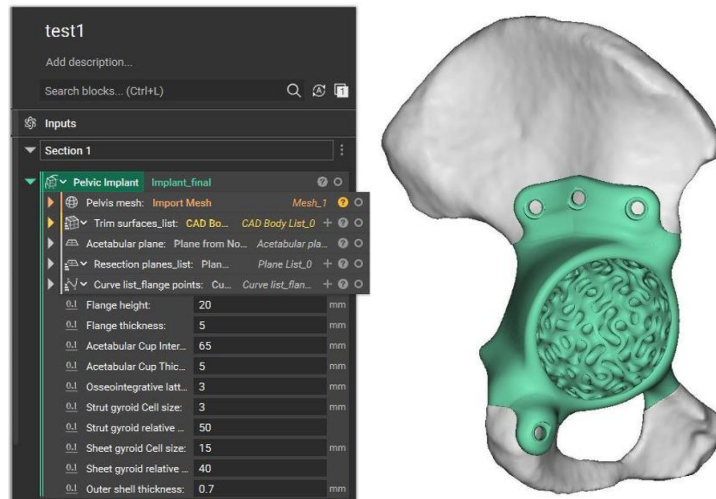


**Figure 10:** Custom block in nTopology for acetabular implants.

The required external inputs, pointed out in Figure 8, are:

- polygonal mesh of the target bone (.STL)
- CAD surfaces to remove the undesired regions (.stp)
- acetabular planes' coordinates and normal (.csv)
- resection planes' coordinates (.csv)
- screws' holes coordinates (.csv)

The procedure requires to type the desired values for the following design variables:

- flange height
- flange thickness
- acetabular cup internal diameter
- acetabular cup thickness
- thickness of the osseointegrative lattice layer
- gyroid cell size for osseointegration
- gyroid relative density for osseointegration
- gyroid cell size for elastic matching at the implant's core
- gyroid relative density at the implant's core

In this case, due to the high variability between each case, the screws' holes are designed separately with a dedicated custom function, allowing to create as many holes as desired with different dimensions.

The workflow enclosed within the custom function implemented in nTopology for the acetabular implant is resumed in Figure 11. The blue blocks represent the operations, while the yellow ones stand for the intermediate results. The dotted lines show at which step each input is involved. Each operation block has been specifically developed and combined to create a robust workflow which exploits the strengths of nTop's implicit modelling engine. First, the pelvis polygonal mesh is converted into implicit representation for further operations; the undesired parts of the pelvis, bounded by the CAD surfaces (e.g. Figure 8 a), are removed, then the result is merged through a Boolean union with the acetabular cup. Since in most cases the original anatomy is not restored, in this framework it is convenient to remove the undesired parts of the pelvis before the process starts to guarantee a better outcome.

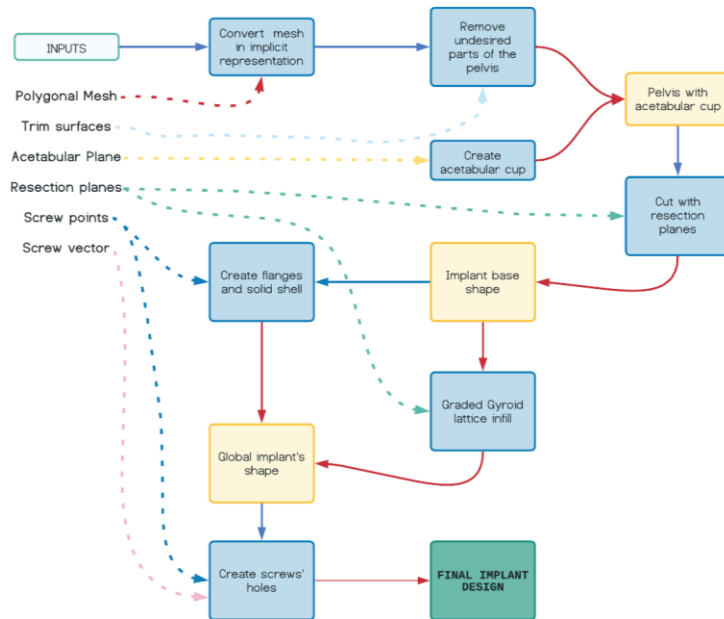


**Figure 11:** Acetabular implant workflow.

#### 4 RESULTS AND DISCUSSION

The robustness and flexibility of algorithms presented have been tested to reproduce 20 case-studies provided by Careggi Hospital regarding the pelvic region. Due to privacy issues, the original images of the actual implants can't be disclosed. The automatic procedure managed to effortlessly reproduce each of the cases analyzed and proved to be very robust. Some examples are reported in Figure 12.

The mean processing time for the 20 case-studies was  $2 \pm 0.15$  minutes on a laptop with GeForce RTX3070 graphic card, AMD Ryzen 9 5900HX processor and 32 Gb RAM. Such result is impressive if compared to the manual processing time which might take up to several hours, according to the complexity. The presented algorithms are non-sensitive to the design variables, and the processing time is only slightly affected by the quality of the original triangular mesh of the pelvis: the smoother it is, the faster becomes the process.

The designed functions have been stressed by imposing a wide variability of the design parameters e.g., acetabular diameter, screw's hole diameter, flange thickness and height. The implicit representation of bodies implemented in nTopology is extremely powerful in managing complex geometries as the gyroid lattice infill and is always able to create fillets between each

part. Figure 13 shows an example where the hole's diameter has been changed from 5mm to 10mm and yet the software managed to adapt.

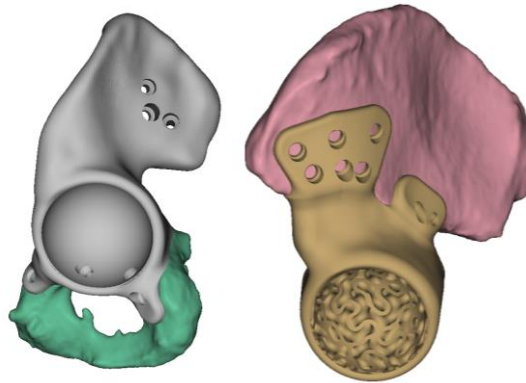


**Figure 12:** Examples of implants designed with the automatic nTopology procedure.

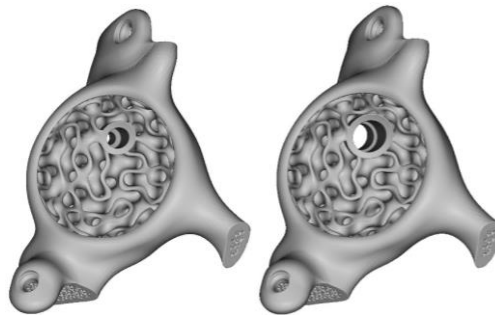


**Figure 13:** Screw hole.

A further example is depicted in Figure 14, where the diameter of the acetabular cup has been set respectively to 50mm, 60mm and 70mm.

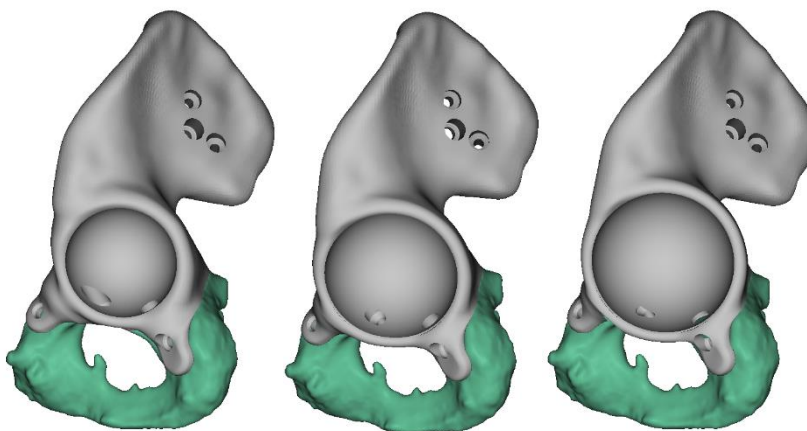


**Figure 14:** Acetabular cup diameter.

The inputs required for the procedure have been manually designed in Geomagic Design X ®, which are:

- resection planes (.csv)
- screw point position (.csv)
- screw vectors, oriented as the screws (.csv)
- CAD surfaces to trim the undesired portions of the original bone (.stp)

The inputs required for the procedure have been manually designed in Geomagic Design X ® and required an average time of  $16 \pm 4.6$  minutes, thus the overall process, from the definition of the inputs to the creation of a ready-to-print 3D model of pelvic implants through the developed algorithm is lower than 20 minutes. Besides the efficiency, the presented workflows also delivers significant advantages in terms of repeatability and product safety, as the human interaction is limited to the input of design variable values, while the CAD operations remain hidden. Furthermore, the user-friendly interface of nTopology enables to design high-performance custom implants with little or no CAD modelling experience, still ensuring a high degree of customization.

To date, the required inputs must be designed into an external software since nTopology, due to its implicit representation of bodies, doesn't allow to easily create CAD entities as surfaces, planes, and points, therefore the presented workflow must be used in conjunction with an external software. Ideally, the required inputs could be exported from a surgical planning software where the surgeons autonomously place resection planes, screws, thus empowering clinicians to have full control over the design and yet retaining the strict design principles enclosed within the automatic workflow.

The procedure proposed in the present paper empowers a competent CAD user with the ability of designing a load-bearing implant with few manual operations. The results are valid in terms of clinical applicability, as confirmed by clinicians of Careggi Florence Hospital. The time required to apply the entire procedure can be estimated in roughly 20 minutes. The use of nTopology modelling architecture has allowed to exploit a procedural modelling logic that has streamlined the entire process and it has permitted the generation and application of complex lattice structures in a limited time.

## ACKNOWLEDGEMENTS

This study was carried out in the context of the PRECISE project "Personalised and pREdictive Surgical Simulation for preCIse tumor resection", financed by Tuscany Region in the "Bando Ricerca & Salute 2018".

## REFERENCES

- [1] Al-Ketan, O.; Rowshan, R.; Abu Al-Rub, R.K.: Topology-mechanical property relationship of 3D printed strut, skeletal, and sheet based periodic metallic cellular materials, *Additive Manufacturing*, 19, 2018, 167–183. <https://doi.org/10.1016/J.ADDMA.2017.12.006>
- [2] Arabnejad, S.; Burnett Johnston, R.; Pura, J.A.; Singh, B.; Tanzer, M.; Pasini, D.: High-strength porous biomaterials for bone replacement: A strategy to assess the interplay between cell morphology, mechanical properties, bone ingrowth and manufacturing constraints, *Acta Biomaterialia*, 30, 2016, 345–356. <https://doi.org/10.1016/J.ACTBIO.2015.10.048>
- [3] Arabnejad, S.; Johnston, B.; Tanzer, M.; Pasini, D.: Fully porous 3D printed titanium femoral stem to reduce stress-shielding following total hip arthroplasty, *Journal of Orthopaedic Research: Official Publication of the Orthopaedic Research Society*, 35, 2017, 1774–1783. <https://doi.org/10.1002/JOR.23445>
- [4] Barba, D.; Alabort, E.; Reed, R.C.: Synthetic bone: Design by additive manufacturing, *Acta Biomaterialia*, 97, 2019, 637–656. <https://doi.org/10.1016/J.ACTBIO.2019.07.049>
- [5] Bezuidenhout, M.B.; Dimitrov, D.M.; Van Staden, A.D.; Oosthuizen, G.A.; Dicks, L.M.T.: Titanium-based hip stems with drug delivery functionality through additive manufacturing,

- BioMed Research International, 2015, 2015. <https://doi.org/10.1155/2015/134093>
- [6] Buonamici, F.; Guariento, L.; Volpe, Y.: 3D Digital Surgical Planning: An Investigation of Low-Cost Software Tools for Concurrent Design, 2020. [https://doi.org/10.1007/978-3-030-31154-4\\_65](https://doi.org/10.1007/978-3-030-31154-4_65)
- [7] Cima, L.G.; Vacanti, J.P.; Vacanti, C.; Ingber, D.; Mooney, D.; Langer, R.: Tissue engineering by cell transplantation using degradable polymer substrates, *Journal of Biomechanical Engineering*, 113, 1991, 143–151. <https://doi.org/10.1115/1.2891228>
- [8] Cootes, T.F.; Edwards, G.J.; Taylor, C.J.: Active appearance models, *Lecture Notes in Computer Science (Including Subseries Lecture Notes in Artificial Intelligence and Lecture Notes in Bioinformatics)*, 1407, 1998, 484–498. <https://doi.org/10.1007/BFB0054760>
- [9] Cootes, T.F.; Taylor, C.J.; Cooper, D.H.; Graham, J.: Active Shape Models-Their Training and Application, *Computer Vision and Image Understanding*, 61, 1995, 38–59. <https://doi.org/10.1006/CVIU.1995.1004>
- [10] Dall’Ava, L.; Hothi, H.; Henckel, J.; Di Laura, A.; Shearing, P.; Hart, A.: Comparative analysis of current 3D printed acetabular titanium implants, *3D Printing in Medicine* 2019 5:1, 5, 2019, 1–10. <https://doi.org/10.1186/S41205-019-0052-0>
- [11] Fuessinger, M.A.; Schwarz, S.; Cornelius, C.P.; Metzger, M.C.; Ellis, E.; Probst, F.; et al.: Planning of skull reconstruction based on a statistical shape model combined with geometric morphometrics, *International Journal of Computer Assisted Radiology and Surgery*, 13, 2018, 519–529. <https://doi.org/10.1007/S11548-017-1674-6>
- [12] Gelaude, F.; Clijmans, T.; Broos, P.L.; Lauwers, B.; Vander Sloten, J.: Computer-aided planning of reconstructive surgery of the innominate bone: automated correction proposals, *Computer Aided Surgery: Official Journal of the International Society for Computer Aided Surgery*, 12, 2007, 286–294. <https://doi.org/10.3109/10929080701684762>
- [13] Griffith, L.G.: Emerging design principles in biomaterials and scaffolds for tissue engineering, *Annals of the New York Academy of Sciences*, 961, 2002, 83–95. <https://doi.org/10.1111/J.1749-6632.2002.TB03056.X>
- [14] Guariento, L.; Buonamici, F.; Marzola, A.; Volpe, Y.; Governi, L.: Graded Gyroid Structures for Load Bearing Orthopedic Implants, *Proceedings of the 2020 IEEE 10th International Conference on “Nanomaterials: Applications and Properties”, NAP 2020*, 2020. <https://doi.org/10.1109/NAP51477.2020.9309692>
- [15] Han, C.; Li, Y.; Wang, Q.; Wen, S.; Wei, Q.; Yan, C.; et al.: Continuous functionally graded porous titanium scaffolds manufactured by selective laser melting for bone implants, *Journal of the Mechanical Behavior of Biomedical Materials*, 80, 2018, 119–127. <https://doi.org/10.1016/J.JMBBM.2018.01.013>
- [16] Heimann, T.; Meinzer, H.P.: Statistical shape models for 3D medical image segmentation: A review, *Medical Image Analysis*, 13, 2009, 543–563. <https://doi.org/10.1016/J.MEDIA.2009.05.004>
- [17] Hua, Z.; Fan, Y.; Cao, Q.; Wu, X.: Biomechanical Study on the Novel Biomimetic Hemi Pelvis Prosthesis, *Journal of Bionic Engineering*, 10, 2013, 506–513. [https://doi.org/10.1016/S1672-6529\(13\)60244-9](https://doi.org/10.1016/S1672-6529(13)60244-9)
- [18] Javaid, M.; Haleem, A.: Additive manufacturing applications in orthopaedics: A review, *Journal of Clinical Orthopaedics and Trauma*, 9, 2018, 202–206. <https://doi.org/10.1016/J.JCOT.2018.04.008>
- [19] Javaid, M.; Haleem, A.: Current status and challenges of Additive manufacturing in orthopaedics: An overview, *Journal of Clinical Orthopaedics and Trauma*, 10, 2019, 380–386. <https://doi.org/10.1016/J.JCOT.2018.05.008>
- [20] Karageorgiou, V.; Kaplan, D.: Porosity of 3D biomaterial scaffolds and osteogenesis, *Biomaterials*, 26, 2005, 5474–5491. <https://doi.org/10.1016/J.BIOMATERIALS.2005.02.002>
- [21] Karande, T.S.; Ong, J.L.; Agrawal, C.M.: Diffusion in Musculoskeletal Tissue Engineering Scaffolds: Design Issues Related to Porosity, Permeability, Architecture, and Nutrient Mixing, *Annals of Biomedical Engineering* 2004 32:12, 32, 2004, 1728–1743. <https://doi.org/10.1007/S10439-004-7825-2>



- [22] Khanoki, S.A.; Pasini, D.: The fatigue design of a bone preserving hip implant with functionally graded cellular material, *Journal of Medical Devices, Transactions of the ASME*, 7, 2013. <https://doi.org/10.1115/1.4024310>
- [23] Liebschner, M.A.K.: Biomechanical considerations of animal models used in tissue engineering of bone, *Biomaterials*, 25, 2004, 1697–1714. [https://doi.org/10.1016/S0142-9612\(03\)00515-5](https://doi.org/10.1016/S0142-9612(03)00515-5)
- [24] Mahmoud, D.; Elbestawi, M.A.: Lattice Structures and Functionally Graded Materials Applications in Additive Manufacturing of Orthopedic Implants: A Review, *Journal of Manufacturing and Materials Processing*, 1, 2017, 13. <https://doi.org/10.3390/JMMP1020013>
- [25] Marzola, A.; Buonamici, F.; Guariento, L.; Governi, L.: Enhanced Statistical Shape Model: A Statistical-Based Tool to design Custom Orthopaedic Devices, *Lecture Notes in Mechanical Engineering*, 2022, 27–38. [https://doi.org/10.1007/978-3-030-91234-5\\_3](https://doi.org/10.1007/978-3-030-91234-5_3)
- [26] Michielsen, K.; Stavenga, D.G.: Gyroid cuticular structures in butterfly wing scales: biological photonic crystals, *Journal of the Royal Society Interface*, 5, 2008, 85. <https://doi.org/10.1098/RSIF.2007.1065>
- [27] Mooney, D.J.; Baldwin, D.F.; Suh, N.P.; Vacanti, J.P.; Langer, R.: Novel approach to fabricate porous sponges of poly(d,l-lactic-co-glycolic acid) without the use of organic solvents, *Biomaterials*, 17, 1996, 1417–1422. [https://doi.org/10.1016/0142-9612\(96\)87284-X](https://doi.org/10.1016/0142-9612(96)87284-X)
- [28] Parithimarkalaigan, S.; Padmanabhan, T. V.: Osseointegration: An Update, *The Journal of the Indian Prosthodontic Society*, 13, 2013, 2. <https://doi.org/10.1007/S13191-013-0252-Z>
- [29] Pellanconi, M.; Ortona, A.: Nature-Inspired, Ultra-Lightweight Structures with Gyroid Cores Produced by Additive Manufacturing and Reinforced by Unidirectional Carbon Fiber Ribs, *Materials* 2019, Vol 12, Page 4134, 12, 2019, 4134. <https://doi.org/10.3390/MA12244134>
- [30] du Plessis, A.; Yadroitsava, I.; Yadroitsev, I.; le Roux, S.G.; Blaine, D.C.: Numerical comparison of lattice unit cell designs for medical implants by additive manufacturing, *Virtual and Physical Prototyping*, 13, 2018, 266–281. <https://doi.org/10.1080/17452759.2018.1491713>
- [31] du Plessis, A.; Broeckhoven, C.; Yadroitsava, I.; Yadroitsev, I.; Hands, C.H.; Kunju, R.; et al.: Beautiful and Functional: A Review of Biomimetic Design in Additive Manufacturing, *Additive Manufacturing*, 27, 2019, 408–427. <https://doi.org/10.1016/J.ADDMA.2019.03.033>
- [32] Taniguchi, N.; Fujibayashi, S.; Takemoto, M.; Sasaki, K.; Otsuki, B.; Nakamura, T.; et al.: Effect of pore size on bone ingrowth into porous titanium implants fabricated by additive manufacturing: An in vivo experiment, *Materials Science and Engineering: C*, 59, 2016, 690–701. <https://doi.org/10.1016/J.MSEC.2015.10.069>
- [33] Vats, A.; Tolley, N.S.; Polak, J.M.; Gough, J.E.: Scaffolds and biomaterials for tissue engineering: a review of clinical applications, *Clinical Otolaryngology and Allied Sciences*, 28, 2003, 165–172. <https://doi.org/10.1046/J.1365-2273.2003.00686.X>
- [34] Vijayavenkataraman, S.; Zhang, L.; Zhang, S.; Fuh, J.Y.H.; Lu, W.F.: Triply periodic minimal surfaces sheet scaffolds for tissue engineering applications: An optimization approach toward biomimetic scaffold design, *ACS Applied Bio Materials*, 1, 2018, 259–269. [https://doi.org/10.1021/ACSABM.8B00052/ASSET/IMAGES/ACSABM.8B00052.SOCIAL.JPEG\\_V03](https://doi.org/10.1021/ACSABM.8B00052/ASSET/IMAGES/ACSABM.8B00052.SOCIAL.JPEG_V03)
- [35] Weinans, H.; Sumner, D.R.; Igloria, R.; Natarajan, R.N.: Sensitivity of periprosthetic stress-shielding to load and the bone density-modulus relationship in subject-specific finite element models, *Journal of Biomechanics*, 33, 2000, 809–817. [https://doi.org/10.1016/S0021-9290\(00\)00036-1](https://doi.org/10.1016/S0021-9290(00)00036-1)
- [36] Yan, C.; Hao, L.; Hussein, A.; Young, P.: Ti–6Al–4V triply periodic minimal surface structures for bone implants fabricated via selective laser melting, *Journal of the Mechanical Behavior of Biomedical Materials*, 51, 2015, 61–73. <https://doi.org/10.1016/J.JMBBM.2015.06.024>
- [37] Yang, E.; Leary, M.; Lozanovski, B.; Downing, D.; Mazur, M.; Sarker, A.; et al.: Effect of

- geometry on the mechanical properties of Ti-6Al-4V Gyroid structures fabricated via SLM: A numerical study, *Materials & Design*, 184, 2019, 108165. <https://doi.org/10.1016/J.MATDES.2019.108165>
- [38] Yang, L.; Mertens, R.; Ferrucci, M.; Yan, C.; Shi, Y.; Yang, S.: Continuous graded Gyroid cellular structures fabricated by selective laser melting: Design, manufacturing and mechanical properties, *Materials & Design*, 162, 2019, 394–404. <https://doi.org/10.1016/J.MATDES.2018.12.007>
- [39] Yang, L.; Yan, C.; Fan, H.; Li, Z.; Cai, C.; Chen, P.; et al.: Investigation on the orientation dependence of elastic response in Gyroid cellular structures, *Journal of the Mechanical Behavior of Biomedical Materials*, 90, 2019, 73–85. <https://doi.org/10.1016/J.JMBBM.2018.09.042>
- [40] Yoo, D.J.: Porous scaffold design using the distance field and triply periodic minimal surface models, *Biomaterials*, 32, 2011, 7741–7754. <https://doi.org/10.1016/J.BIOMATERIALS.2011.07.019>
- [41] Yoo, D.J.: Advanced porous scaffold design using multi-void triply periodic minimal surface models with high surface area to volume ratios, *International Journal of Precision Engineering and Manufacturing* 2014 15:8, 15, 2014, 1657–1666. <https://doi.org/10.1007/S12541-014-0516-5>
- [42] Yousaf, M.N.; Houseman, B.T.; Mrksich, M.: Using electroactive substrates to pattern the attachment of two different cell populations, *Proceedings of the National Academy of Sciences of the United States of America*, 98, 2001, 5992–5996. <https://doi.org/10.1073/PNAS.101112898/ASSET/34DA6D45-A3ED-4D6C-A167-E3366EB665A0/ASSETS/GRAPHIC/PQ1011128005.JPEG>
- [43] Zaharin, H.A.; Rani, A.M.A.; Azam, F.I.; Ginta, T.L.; Sallih, N.; Ahmad, A.; et al.: Effect of Unit Cell Type and Pore Size on Porosity and Mechanical Behavior of Additively Manufactured Ti6Al4V Scaffolds, *Materials*, 11, 2018, . <https://doi.org/10.3390/MA1122402>
- [44] Zhang, B.; Pei, X.; Zhou, C.; Fan, Y.; Jiang, Q.; Ronca, A.; et al.: The biomimetic design and 3D printing of customized mechanical properties porous Ti6Al4V scaffold for load-bearing bone reconstruction, *Materials & Design*, 152, 2018, 30–39. <https://doi.org/10.1016/J.MATDES.2018.04.065>
- [45] Zhang, X.Y.; Fang, G.; Zhou, J.: Additively Manufactured Scaffolds for Bone Tissue Engineering and the Prediction of their Mechanical Behavior: A Review, *Materials (Basel, Switzerland)*, 10, 2017. <https://doi.org/10.3390/MA10010050>
- [46] Next-Generation Engineering Design Software | nTopology, n.d., . <https://ntopology.com/> (accessed: 04/05/2022)